Stratospheric Impact of Two Types of El Niño Events in WACCM3.5 simulations

Isabel Zubiaurre (1), Natalia Calvo (1), (2)

(1) Universidad Complutense de Madrid (2) ACD NCAR Boulder, Colorado

izubiaurre@gmail.com

Motivation

El Nino-Southern Oscillation (ENSO) :

- Largest source of interannual variability in the tropical troposphere.
- ENSO signal propagates upwards into the stratosphere and has an effect in tropics and NH polar stratosphere region.
- Since 1979, the variability in the tropical Pacific is associated not only to the canonical ENSO, but also to a new phenomenon referred as **ENSO Modoki** [Ashok et al., 2007].
- This new phenomenon has **different** frequency, magnitude and localization of the SSTA (Figure 1) in the tropical Pacific, leading to different tropospheric teleconnection patterns.

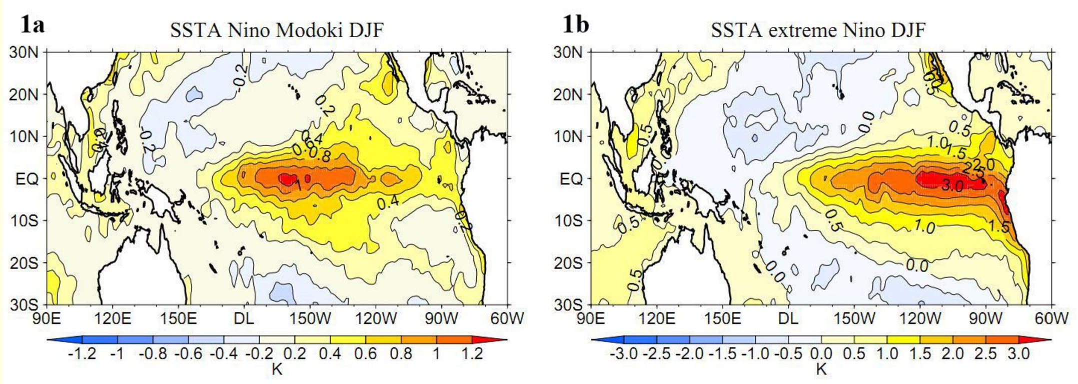

Figure 1. SSTA composites for a) El Niño Modoki and b) extreme Canonical El Niño events for DJF from 1979 to 2004.

Objective: to characterize and understand the impact of this new phenomenon in the **stratosphere** and to compare it with Canonical El Niño

Data and Method

❑ **WACCM3.5:** The Whole Atmosphere Community Climate Model :

- Resolves the atmosphere vertically from the surface to 140 km.
- It is based on version 3 of the Community Atmospheric Model (CAM) .
- Incorporates most of the physical and chemical processes required to model the middle atmosphere.
- Four-member ensemble simulations run for 1953-2004
  [simulations are part of the second CCM validation activity (CCMVal2) of the SPARC project [SPARC CCMVal, 2010]].
- Horizontal resolution: 1.98 latitude x 2.58 longitude.
- Sea surface temperatures (SST) are prescribed from observed data [MetOffice Hadley Center [Rayner et al., 2006]].
- Monthly-mean ensemble series were deseasonalized and then regressed onto different predictors using a **multivariate linear regression**. It includes terms to account for the long-term trend, the 11-yr solar cycle, the QBO, and the effects of volcanic eruptions. The **residual** contains the ENSO signal. The residual series is smoothed to eliminate subseasonal fluctuations. This final product is the series we have used in the analysis of the ENSO signal.
- Analyzed period: 1979-2004.
- Composites computed for strong El Niño Modoki and extreme Canonical El Niño events.

❑ **El Niño Modoki index (EMI)** characterizes El Niño Modoki events [Ashok et al., 2007]:

EMI = [SSTA] $_A$ - 0.5 [SSTA] $_B$ - 0.5[SSTA] $_C$

❑ **Niño3 index (N3)** characterizes the Canonical El Niño.

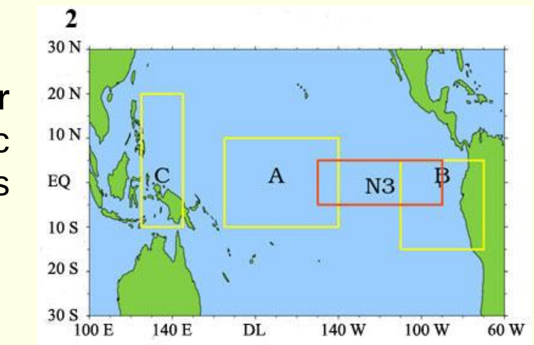

Figure 2. Representation of the regions employed to calculate EMI index (A, B and C boxes) and N3 index.

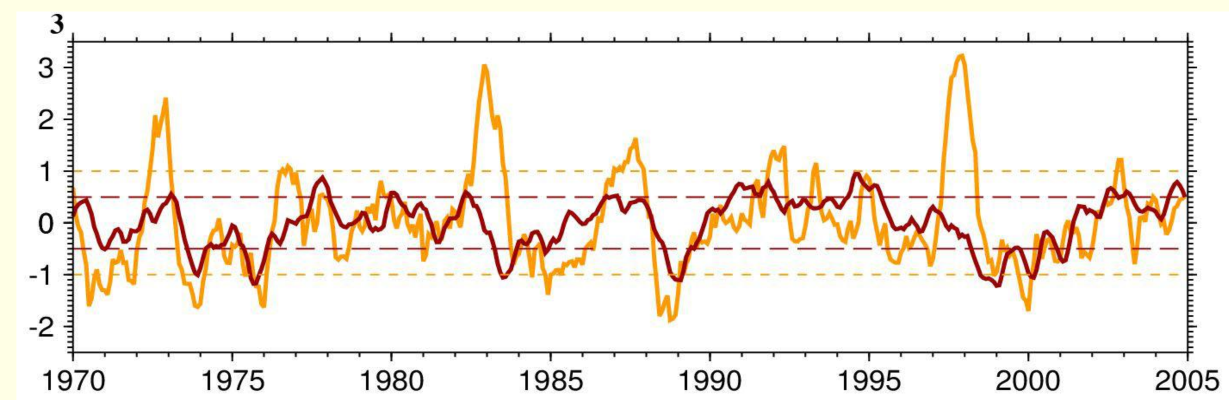

NIÑO MODOKI		EXTREME NIÑO 3	
EVENT	**EMI**	**EVENT**	**N3**
February1980	0.5628	December 1972	2.4388
February 1987	0.5052	December 1982	3.0789
January 1991	0.7042	December 1997	3.2506
November 1991	0.7269		
August 1994	0.8958		
February 2003	0.5837		

✓ In the composites, the significance of the anomalies with respect to the internal variability of each data set has been tested by a **Monte Carlo** method (in color in Figures).

Figure 3 (left). EMI (thick red line) and N3 (thick orange line) index after being smoothed.

Table 1. Maximum values of EMI for El Niño Modoki events (left) and N3 for extreme Canonical El Niño events (right).

Stratospheric Niño Modoki Signal

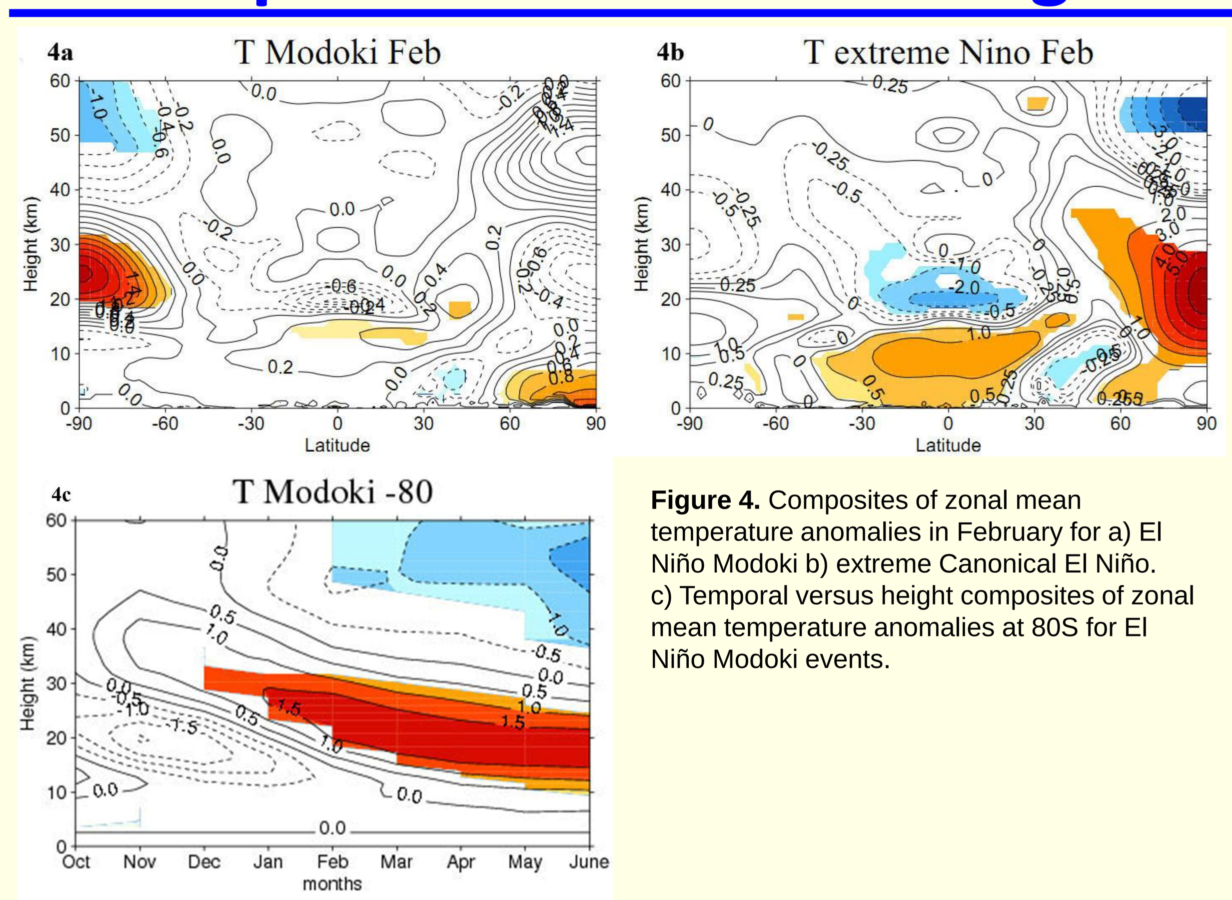

Figure 4. Composites of zonal mean temperature anomalies in February for a) El Niño Modoki b) extreme Canonical El Niño. c) Temporal versus height composites of zonal mean temperature anomalies at 80S for El Niño Modoki events.

❑ **SH:** A **significant warming** in the SH polar stratosphere during El Niño Modoki events, not observed during Canonical ENSO episodes **+** a weakening of the SH polar vortex and a significant increase in ozone anomalies (not shown)

❑ **NH:** N**o significant signal** during El Niño Modoki events (despite Canonical ENSO events have their largest impact in the NH polar stratosphere.)

❑ **SUBTROPICS:** the anomalous warming/cooling in the upper troposphere/low stratosphere is **weaker and not as persistent** as during Canonical El Niño events. Related to the weaker anomalies in SST generated by El Niño Modoki events compared to Canonical El Niño ones.

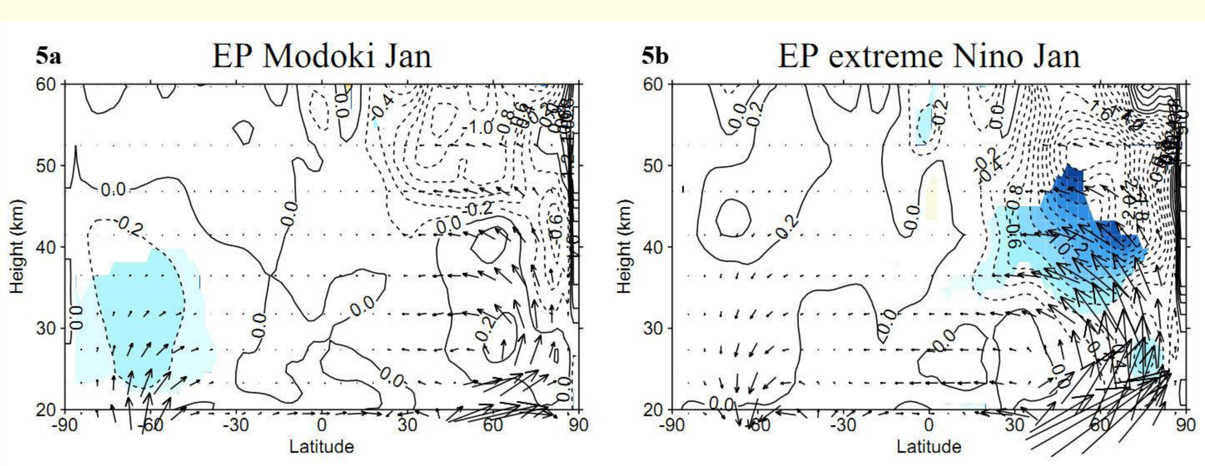

Figure 5. Composites of Eliassen Palm (EP) flux (arrows) and EP flux divergence (shadowed) anomalies in January for a) El Niño Modoki b) extreme Canonical El Niño.

❑ **SH: Significant upward wave propagation at high latitudes** during El Niño Modoki causes dissipation of the waves in the middle stratosphere (not seen during Canonical El Niño).

❑ **NH:** Upward wave propagation at high latitudes for both phenomena, but there is **no significant wave forcing** during El Niño Modoki → no significant impact on the mean flow and on temperature (Figure 4).

Mechanisms: tropical forcing

A) Differences in teleconnection patterns:

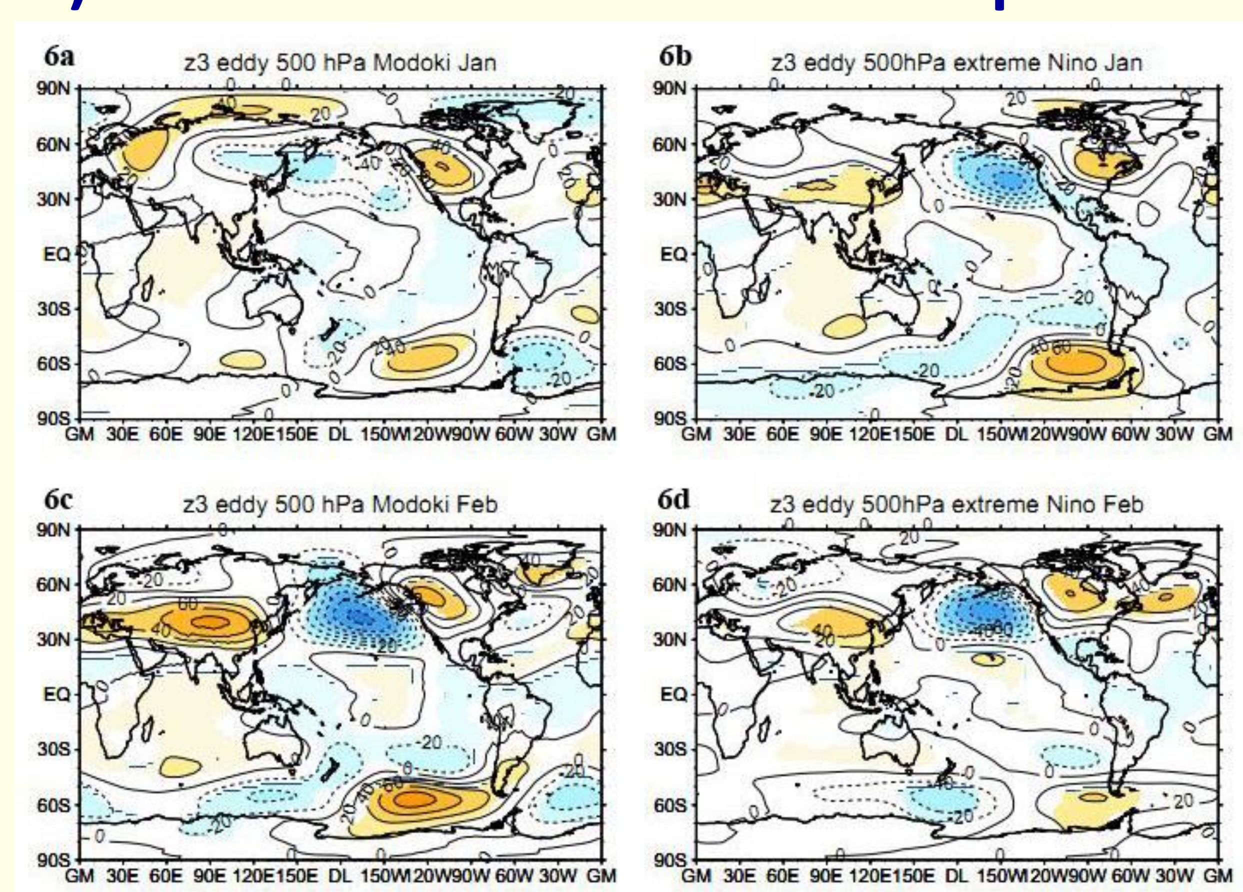

Figure 6. Composites of geopotential height eddy anomalies at 500 hPa in January and February for a) El Niño Modoki and b) Canonical extreme Canonical El Niño.

✓ Main tropospheric extratropical ENSO teleconnections: Pacific North American pattern (PNA) and Pacific South American pattern (PSA).

❑ **SH: A stronger PSA** teleconnection pattern is simulated during El Niño Modoki

❑ **NH:** the **PNA** teleconnection pattern appears later in the winter (compared to Canonical El Niño) and with the Aleutian Low weaker until February.

✓ **The intensification and duration of the teleconnection patterns depend on the type of event**.

✓PSA modes are associated with changes in convection in the Tropical Pacific Ocean [Mo and Higgins, 1998]

✓ Convection intensifies in both cases in the tropical Pacific, **being larger for El Niño Modoki** than for Canonical El Niño. However, their longitudinal extension is very different: convection anomalies **extend westward exceeding the Dateline** for El Niño Modoki; while they appear east of the Dateline for Canonical El Niño (Figure 7).

✓ **This difference in the convection location between the two phenomena is the main reason of the different teleconnections between them.**

B) Differences in convection patterns:

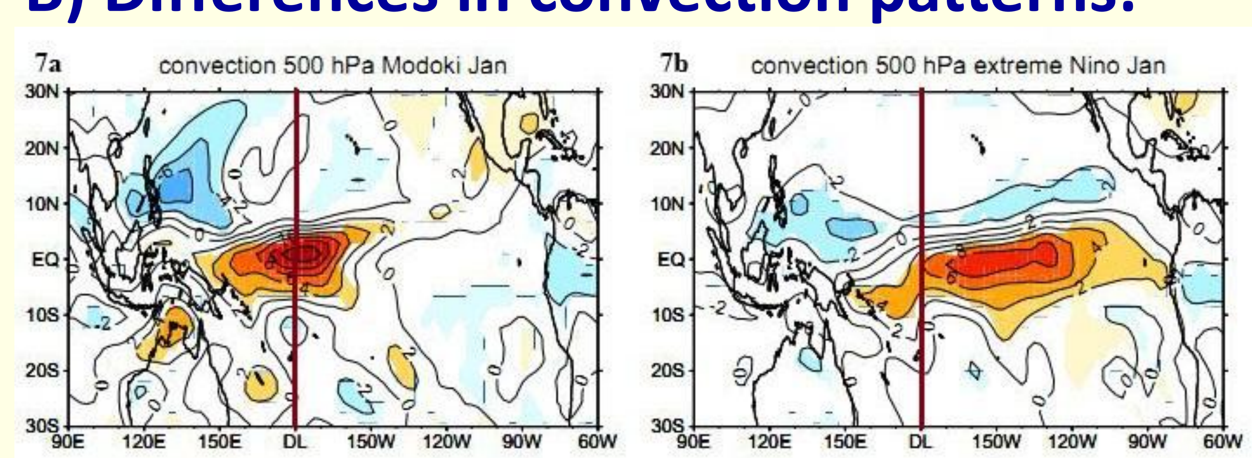

Figure 7. Composites of convection heating rates anomalies at 500 hPa in January for a) El Niño Modoki and b) Canonical extreme Canonical El Niño.

✓ **A westward displacement and larger convection anomalies during El Niño Modoki events lead to an intensification of the PSA. At high latitudes of the SH, waves propagate upwards to the stratosphere.**

This upward propagation is also seen in the geopotential height eddy anomalies at 60 S (Figure 8b). The climatology shows that there is upward propagation of the waves (Figure 8a). El Niño Modoki events (Figure 8b) **interferes more constructively** with the climatology than Canonical El Niño events (Figure 8c) because of the longitudinal location of positive and negative anomalies, in relation to the location of the SSTA in both events (Figure 1).

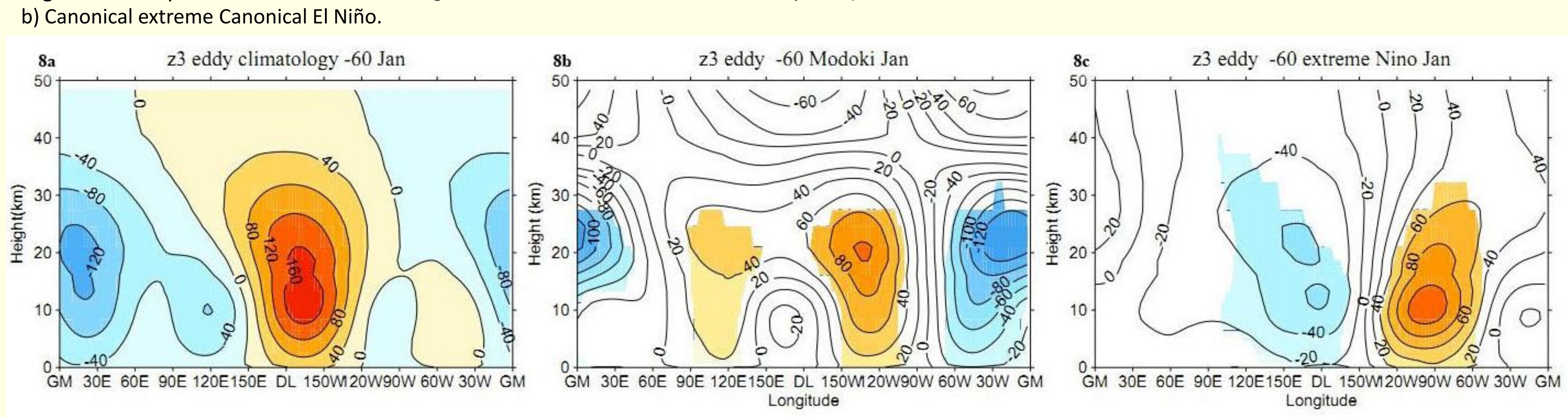

Figure 8. a-b) Geopotential height eddy climatology and c-f) composites of eddy geopotential height anomalies for c-d) El Niño Modoki e-f) Canonical El Niño at 60 S in December and January

Conclusions

West and larger convection during El Niño Modoki events → **PSA intensification** → Upward wave propagation → Rossby waves reach the stratosphere, they decelerate the mean flow and cause **a weakening of the polar vortex and a warming of the Southern Polar stratosphere**

Aleutian Low of the PNA is weaker for El Niño Modoki → **Waves that propagate upwards into the stratosphere do not produce any significant forcing in the region** → No significant warming in the Northern Polar stratosphere

References and Acknowledgments

- Ashok K., S. Behera, A.S. Rao, H.Y. Weng, and T. Yamagata (2007), El Niño Modoki and its teleconnection, J.Geophys. Res., 112, C11007.
- García-Herrera R., N. Calvo, R.R. García, and M.A. Giorgetta (2006), Propagation of ENSO temperature signals into the middle atmosphere: a comparison of two general circulation models and ERA-40 reanalysis data , J.Geophys. Res., 111, D06101.
- Mo K.C. and R.W. Higgins (1998), The Pacific–South American Modes and Tropical Convection during the Southern Hemisphere Winter, Mon. Wea. Rev., 126, 1581-1596.
- Rayner N.A., D.E. Parker, E.B. Horton, C.K. Folland, L.V. Alexander, D.P. Rowell, E.C. Kent, and A. Kaplan (2003), Global analyses of sea surface temperature, sea ice, and night marine air temperature since the late nineteenth century, J.Geophys. Res., 108 4407-4444.
- SPARC CCMVal (2010), SPARC Report on the Evaluation of Chemistry-Climate Models, V. Eyring, T. G. Shepherd, D. W. Waugh (Eds.), SPARC Report No. 5, WCRP-132, WMO/TD-No. 1526, http://www.atmosp.physics.utoronto.ca/SPARC.

❑ This research was supported by the Ministry of Science and Innovation of Spain under the project TRODIM (CGL2007-65891-C05-02).